Research Square

Preprints are preliminary reports that have not undergone peer review.
They should not be considered conclusive, used to inform clinical practice,
or referenced by the media as validated information.

Synergistic Sequential Phosphoric Acid-Deep Eutectic Solvent Pretreatment-Based Biorefinery: Selective Fractionation of Sugarcane Bagasse and Isolation of Structurally Preserved Lignin

Md. Rashed Hasan
Bangladesh Council of Scientific & Industrial Research
Nigar Fatima
National Institute of Biotechnology
Sonia Akter
Bangladesh Council of Scientific & Industrial Research
Md. Saiful Islam
Bangladesh Council of Scientific & Industrial Research
Md. Farid Ahmed
Bangladesh Council of Scientific & Industrial Research
Mohammad Majedul Haque
Bangladesh Council of Scientific & Industrial Research
S. M. Asaduzzaman Sujan
Bangladesh Council of Scientific & Industrial Research
Swapan Kumer Ray
swapanray_bcsir@ymail.com

Bangladesh Council of Scientific & Industrial Research

Research Article

Keywords: Lignocellulosic biomass fractionation, Sugarcane bagasse, Deep eutectic solvent, Sequential acid-DES pretreatment, Lignin extraction and valorization, Cellulose recovery and crystallinity

Posted Date: July 8th, 2026

DOI: https://doi.org/10.21203/rs.3.rs-9502841/v1

License: This work is licensed under a Creative Commons Attribution 4.0 International License.
Read Full License

Additional Declarations: No competing interests reported.

Synergistic Sequential Phosphoric Acid-Deep Eutectic Solvent Pretreatment-Based Biorefinery: Selective Fractionation of Sugarcane Bagasse and Isolation of Structurally Preserved Lignin

Md. Rashed Hasan[a], Nigar Fatima[b], Sonia Akter[a], Md. Saiful Islam[a], Md. Farid Ahmed[a], Mohammad Majedul Haque[a], S. M. Asaduzzaman Sujan[a], Swapan Kumer Ray[a*]

[a]Bangladesh Council of Scientific & Industrial Research, Dhanmondi, Dhaka, Bangladesh

[b]National Institute of Biotechnology, Savar, Dhaka, Bangladesh

Corresponding author's email: swapanray_bcsir@ymail.com

Abstract

The development of selective and sustainable fractionation strategies is critical for advancing lignocellulosic biorefineries. In this study, a synergistic sequential pretreatment approach combining dilute phosphoric acid (PA) and a choline chloride-lactic acid deep eutectic solvent (*ChCl-LA* DES) was developed for efficient fractionation of sugarcane bagasse (SCB). The initial PA treatment selectively removed ~93% of hemicellulose while enhancing cellulose accessibility and lignin extractability. Subsequent DES treatment enabled over 93% lignin recovery and yielded more than 45 wt% cellulose-rich pulp (*DES-cellulose*) containing ~84% α-cellulose. The *ChCl-LA* DES system was characterized using physicochemical and thermal analyses, confirming its suitability as a stable and effective lignin-solubilizing medium. The recovered *DES-lig*nin exhibited nanoscale features, as evidenced by dynamic light scattering (DLS) and scanning electron microscopy (SEM). Detailed structural characterization using heteronuclear single quantum coherence nuclear magnetic resonance (HSQC-NMR) spectroscopy revealed the preservation of key native lignin linkages (e.g., β-O-4) and the presence of derivatized structures, indicating minimal condensation during pretreatment. This structural integrity highlights the advantage of the sequential *PA-DES* strategy over conventional approaches that often degrade lignin. X-ray diffraction (XRD) analysis of the cellulose-rich fraction demonstrated disruption of hydrogen bonding and reduced crystallinity, supporting improved downstream processability. Overall, the proposed sequential pretreatment enables controlled and selective deconstruction of lignocellulosic biomass using environmentally benign solvents, achieving high component recovery while preserving lignin functionality. This work provides a promising and scalable pathway for integrated biorefinery applications and lignin valorization.

Keywords: Lignocellulosic biomass fractionation, Sugarcane bagasse, Deep eutectic solvent, Sequential acid-DES pretreatment, Lignin extraction and valorization, Cellulose recovery and crystallinity

1. Introduction

The lignocellulosic biorefinery concept has emerged as a cornerstone of sustainable development by enabling the utilization of abundant and renewable biomass resources, including agricultural residues, forestry waste, and dedicated energy crops [1, 2]. This approach not only reduces reliance on finite fossil resources but also facilitates the conversion of low-value waste streams into high value products such as biofuels, biochemicals, and biomaterials, thereby promoting a circular bioeconomy. By substituting petroleum derived inputs with biobased alternatives, lignocellulosic biorefineries contribute significantly to lowering greenhouse gas emissions and mitigating climate change impacts [3-5].

Despite these advantages, lignocellulosic biomass presents considerable challenges due to its inherent heterogeneity. Variations in chemical composition, e.g., differing proportions of extractives, cellulose, hemicellulose, and lignin, as well as moisture and ash content, complicate process standardization and optimization [6]. A major obstacle lies in the natural recalcitrance of plant cell walls, which necessitates an effective pretreatment step to enable downstream conversion. Conventional pretreatment methods, including steam explosion, dilute acid or alkali hydrolysis, and more recent solvent based systems such as ionic liquids (ILs) and deep eutectic solvents (DESs), have shown effectiveness in disrupting biomass structure. However, these approaches often require high energy input, involve corrosive reagents, or rely on expensive solvents, thereby limiting their large scale applicability [7].

Moreover, existing pretreatment strategies frequently fail to achieve selective and complete fractionation of the primary biomass components, i.e., cellulose, hemicellulose, and lignin (Table 1). In many cases, these processes also lead to the generation of inhibitory compounds, including furfural, hydroxymethylfurfural (HMF), phenolic derivatives, and various extractives such as resins, pigments, and waxes. These inhibitors can significantly hinder microbial fermentation and enzymatic processes, ultimately reducing overall biorefinery efficiency [8]. Additional limitations arise during the enzymatic hydrolysis stage, where the use of commercial cellulases and hemicellulases is constrained by high costs and susceptibility to end product inhibition. Even after pretreatment, insufficient substrate accessibility often remains a bottleneck, leading to suboptimal sugar yields [9].

Table 1 Some pretreatment strategies aim to facilitate the efficient recovery of the primary structural components from different lignocellulosic biomass

Pretreatment type	Common process agents	Mechanism	Challenges	Lignin quality	Present status
Sequential acid-KOH	Phosphoric acid + KOH	Acid hydrolysis of hemicellulose + KOH delignification	Integrated, recyclable, mild corrosion	High	Reported [16]
Dilute acid	H_2SO_4, HCl	Hemicellulose hydrolysis	Corrosive, inhibitors	Condensed, degraded	Well studied [17, 18]
Phosphoric acid	H_3PO_4	Hemicellulose solubilization, swelling cellulose	Milder, but less selective on lignin	Moderate	
Alkaline pretreatment	NaOH, KOH	Lignin solubilization	Chemical recovery needed	Moderate to high	Established [19]
Organosolv	(MeOH + acid), (EtOH + acid)	Lignin solubilization	Flammable solvents, expensive	High	Known but niche [20]
Ionic liquid	[Emim][OAc], [Bmim][Cl]	Cellulose solubilization, partial solubilization of hemicellulose and lignin	Cost, toxicity, recyclability	Moderate to high	Emerging [21]
DES-only	*ChCl-LA*, ChCl-Urea	Selective lignin solubilization	High viscosity, recyclability issues	Moderate to high	Emerging [22]
Sequential acid-DES	Phosphoric acid + *ChCl-LA* DES	Acid hydrolysis of hemicellulose + DES delignification	Not reported	Not reported	Not reported

Another critical issue is the underutilization of lignin, which typically accounts for 15-30% of lignocellulosic biomass. Despite its abundance and potential as a renewable feedstock, lignin is often relegated to combustion for process heat. This practice overlooks its significant value as a precursor for advanced materials such as phenolic resins, adhesives, and carbon based products [10]. Structurally, lignin is a complex and heterogeneous biopolymer composed of three primary monolignols, i.e., p-coumaryl alcohol, coniferyl alcohol, and sinapyl alcohol (Fig. 1) [11]. These monomers undergo enzyme mediated dehydrogenative polymerization within the plant cell wall, forming a highly crosslinked and recalcitrant network (Fig. 2a).

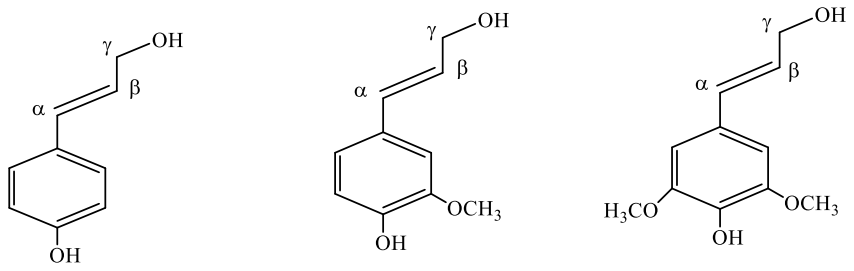


Fig. 1 Three main precursors of lignin, i.e., monolignols

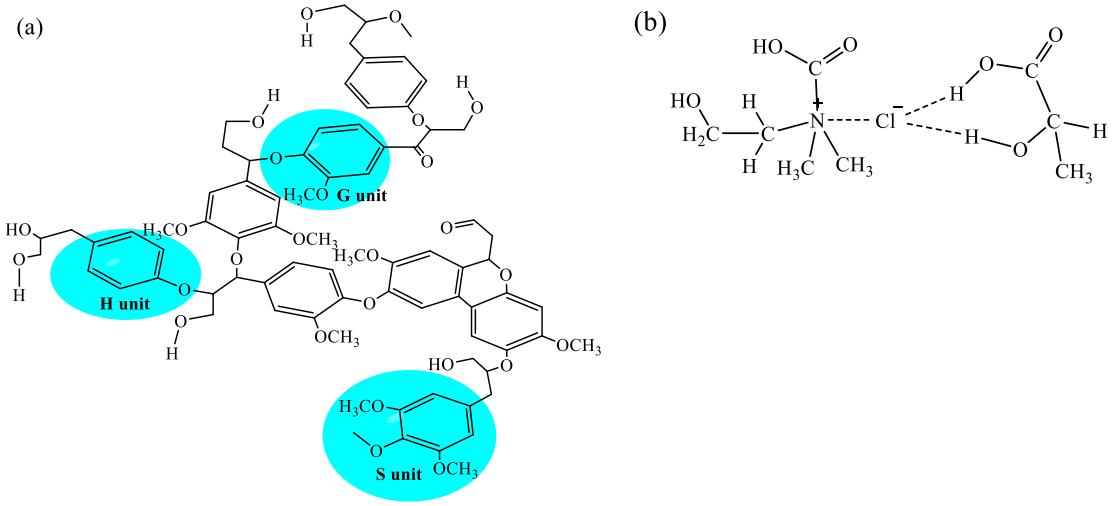


Fig. 2 (a) Partial structure of lignin and (b) Hydrogen bonding in *ChCl-LA* DES system

The structural complexity of lignin arises from a variety of inter-unit linkages, including β-O-4, α-O-4, β-5, β-1, 4-O-5, 5-5, and β-β bonds, which collectively contribute to its chemical stability and resistance to microbial degradation [12-14]. In addition, lignin contains diverse functional groups, e.g., aliphatic and phenolic hydroxyls, carbonyl, carboxyl, and methoxyl groups that influence its reactivity and potential for downstream applications [15]. These structural and functional variations depend strongly on the biomass source and extraction method, making lignin both versatile and challenging to characterize comprehensively.

Addressing these challenges requires an integrated and strategic approach that combines efficient pretreatment with effective component valorization. Recent efforts have focused on designing streamlined and technoeconomically viable biorefinery systems capable of

sequentially recovering both nonstructural and structural components from diverse biomass feedstocks [16]. In this context, the present study proposes a synergistic sequential pretreatment strategy involving PA hydrolysis followed by treatment with a *ChCl-LA* DES system (Fig. 2b). This methodology is applied to extractive-free SCB and represents a promising yet relatively underexplored direction in lignocellulosic biorefinery research. While PA and DES-based pretreatments have been studied independently, their sequential integration remains limited in the literature.

Within this framework, PA serves to swell the cellulose matrix, solubilize hemicellulose, and enhance the accessibility of lignin for subsequent DES treatment. The *ChCl-LA* DES system further facilitates lignin solubilization through a combination of intra and intermolecular hydrogen bonding interactions along with other secondary forces (Fig. 3).

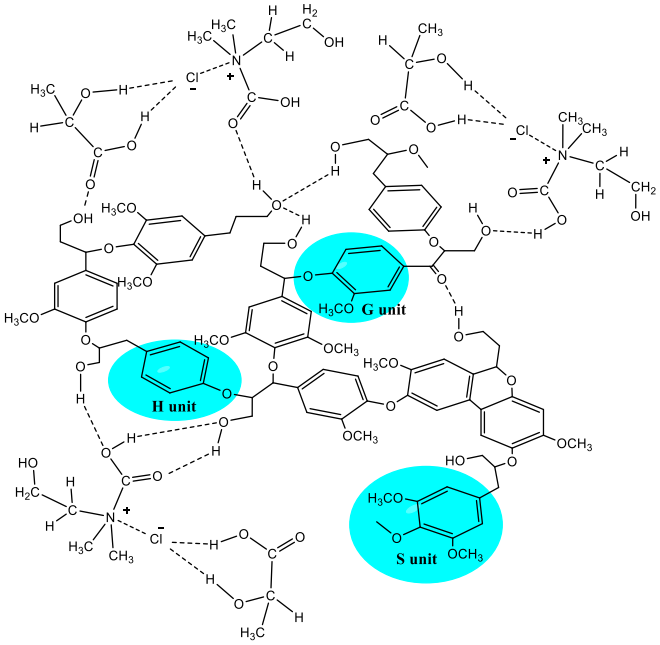


Fig. 3 Lignin macromolecule solvated by *ChCl-LA* DES system through different intra and intermolecular hydrogen bonding and other secondary forces

Beyond enabling stepwise fractionation of hemicellulose and cellulose, the process emphasizes the isolation and detailed characterization of DES-extracted lignin. Comprehensive analyses were conducted, including elemental composition, particle size distribution, functional group identification, overtone and combination band analysis, detailed structural elucidation

through ^{1}H, ^{13}C and ^{1}H-^{13}C HSQC-NMR spectroscopy, thermal behavior assessment, and intrinsic viscosity measurement. Overall, this strategy offers a selective and sustainable pathway for biomass fractionation, with significant potential to enhance the valorization of all major biomass components within an integrated biorefinery framework.

2. Materials and methods

2.1 Materials

Sugarcane bagasse (SCB) was collected from Pabna Sugar Mills Ltd., Bangladesh. Phosphoric acid (Alfa Aesar, India, 85%), ethanol (Merck, Germany, >95%), choline chloride (Assay, dry material: 98.0-100.5%; Research-lab, India), L-lactic acid (Commercial grade; water content 12%), potassium hydroxide (>85%, BDH, UK), dimethylsulfoxide (HPLC grade; Sigma-Aldrich), tetrahydrofuran (HPLC grade; Sigma-Aldrich), commercial cellulose (Merck, India), Activated carbon (BDH, UK), Deionized water (18 MΩ) (MRC deionized water plant, UK) were purchased and used as received to perform overall experiment.

2.2 Methods

The compositional analysis of SCB was conducted using standard analytical methods, as detailed in Supplementary Information (SI) Section S1 and Table S1).

Preparation of ChCl-LA DES system

To prepare a *ChCl-LA* DES, *ChCl* and *LA* in the target molar ratio (1:2.5) was taken in a reagent bottle. The mixture is stirred at 300 rpm at around 60 °C until it became a clear, homogeneous liquid. Once formed, the DES was cooled and stored at room temperature for analysis.

Development of synergistic sequential PA/ ChCl-LA DES-based biorefinery system

The following steps were performed to develop the PA/*ChCl-LA* DES-based biorefinery system to facilitate the production of *DES-lignin* along with the recoveries of extractives, hemicellulose and *DES-cellulose*/pulp from SCB:

Step 1: Reduction of particle size of SCB

Oven-dried SCB was subjected to ball milling operation to reduce the particle size. Powdered SCB of around 100 meshes was used in the work.

Step 2: Removal of water and ethanol soluble extractives

Moisture-free 50g of SCB powder was kept in Soxhlet apparatus. The sample was then subjected to exhaustive extractions with deionized water followed by 95% ethanol in order to remove water and ethanol soluble extractives, respectively. Solvents were driven off from the filtrate to get the extractives by means of distillation apparatus and stored for further analysis. The residue was then dried in oven at 105 ºC until constant weight achieved. Percentage of total extractives was calculated by Equation 1-

$$\%\text{Extractives} = \frac{\text{Weight of residue}}{\text{Weight of sample}} \text{ x } 100 \qquad (1)$$

Step 3: Isolation of hemicellulose from SCB by phosphoric acid pretreatment

Around 35g of extractive-free SCB was pretreated with 2% phosphoric acid solution at 160 ± 10 ºC for 2h maintaining the sample to acid ratio of 15 [16]. An air tight custom made stainless steel digester (SS-316, 1L, Bangladesh) was used for this purpose. After cooling, the slurry was filtered by Gooch type II crucible and washed three times with deionized water up to filtrate volume 1L and then neutralized by potassium hydroxide. The residue was then dried in oven at 105 ºC until constant weight achieved. Percentage of hemicellulose was calculated by Equation 2:

$$\%\text{Hemicellulose} = \frac{\text{Weight of residue}}{\text{Weight of extractive} - \text{ free sample}} \text{ x } 100 \qquad (2)$$

After neutralization with potassium hydroxide solution, hemicellulose containing filtrate was stored for analysis and applications [16]. The extractives and hemicellulose-free SCB is used as feedstock for the pretreatment with *ChCl-LA* DES system.

Step 4: Isolation of DES-lignin from extractives and hemicellulose-free SCB

Around 2.5g of extractives and hemicellulose-free SCB was taken in a reagent bottle and then *ChCl-LA* DES solution was added at sample to solvent ratio of 15. After heating at 90 ± 5 ºC for

6h, the slurry was centrifuged and washed the residue with acetone. The residue, i.e., *DES-cellulose* was stored for analysis. DES containing liquor was collected and vacuum distilled to recover acetone. Finally, deionized water was added into the liquor and subsequently recovered the lignin (i.e., *DES-lignin*) by centrifugation, washed several times with deionized water, vacuum dried until constant weight achieved and then stored. Percentage of *DES-lignin* was calculated by Equation 3. The filtrate was stored to recover the *ChCl-LA* DES.

$$\%DES-lignin = \frac{\text{Weight of acid pretreated sample} - \text{Weight of cellulosic pulp}}{\text{Weight of acid pretreated sample}} \text{ x } 100 \quad (3)$$

Step 5: Recovery of ChCl-LA DES from the system

The filtrate obtained from *Step 4* (contains *ChCl-LA* DES, water, monomeric and oligomeric sugars, and degraded lignin fragments, etc.) was treated with a fourfold excess of cold acetone to induce the precipitation of sugars and lignin-derived impurities. The precipitated solids were recovered using a vacuum filtration unit equipped with a 0.45 μm membrane. To further purify the filtrate, 0.5 g of activated charcoal was mixed with the solution to adsorb color materials and trace organic contaminants, followed by an additional vacuum filtration step. Finally, residual water was removed from the purified *ChCl-LA* DES rich solution by vacuum distillation and preserved for further works.

Effects of extractives and phosphoric acid pretreatment on the isolation of DES-lignin

To investigate the effect of extractives and dilute phosphoric acid pretreatment on the isolation of *DES-lignin*, raw, extractive-free, and extractive-free acid pretreated SCB samples (around 2.5g) were taken in reagent bottles and heated at 90 ± 5 ºC for 6h following the procedure as described earlier. The recovered *DES-lignin* samples were recovered, washed and then dried under vacuum. Detailed procedure was the same as discussed in *Step 4* of the biorefinery system.

The physicochemical properties of the *ChCl-LA* DES system, including moisture content, pH, density, refractive index, viscosity, and thermal behavior, are described in SI Section S2. The physicochemical properties of *DES-lignin* were systematically evaluated using a range of

analytical techniques, including elemental analysis (EA), dynamic light scattering (DLS), scanning electron microscopy (SEM), Fourier transform mid and near infrared (FT-MIR-NIR) spectroscopy, nuclear magnetic resonance (NMR) spectroscopy, simultaneous thermal analysis (STA), and dilute solution viscometry (DSV). In addition, the crystallinity of *DES-cellulose* was examined by X-ray diffraction (XRD) analysis. Detailed experimental procedures are provided in SI Section S3. A schematic representation of the synergistic sequential PA/*ChCl-LA* DES-based lignocellulosic biorefinery system is presented in Fig. 4.

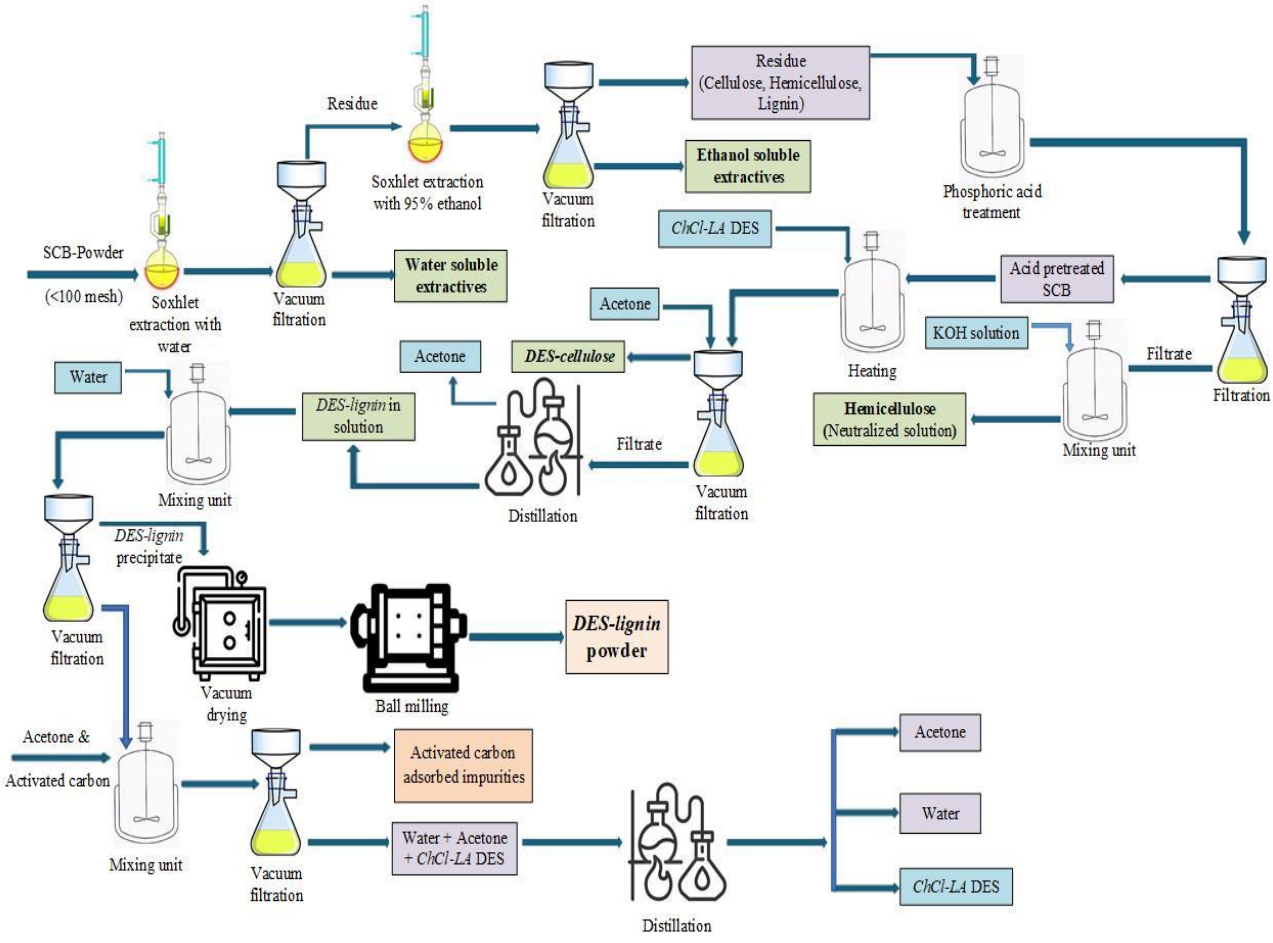


Fig. 4 Schematic diagram of PA/*ChCl-LA* DES-based lignocellulosic biorefinery system

3. Results and discussion

Physicochemical properties of the ChCl-LA DES system

Physicochemical properties, e.g., moisture content, pH, density, and refractive index of *ChCl-LA* DES were investigated and presented in Table 2**.** Viscosity of the DES at different temperatures and variable shear rates are given in Fig. 5**.** The thermograms obtained from simultaneous thermal analyses, e.g., thermogravimetric analysis (TGA and DTG), and differential scanning calorimetric analysis (DSC and DDSC) are presented in Fig. 6**.**

The DES system exhibited a notably low pH at 25 °C, consistent with previous reports on *ChCl-LA* DES formulations [23, 24]. Furthermore, the measured density and refractive index values of the *ChCl-LA* DES were in good agreement with those reported in earlier study [25].

Table 2 Physical properties of *ChCl-LA* DES system

DES	Water content (%)	pH	Density (g/mL)	Refractive index, n_D
		25 °C	25 °C	25 °C
ChCl-LA	12.99	1.6	1.227	1.432

The presence of ~13% water into the *ChCl-LA* DES markedly lowers its dynamic viscosity at ambient temperature, consistent with previous reports [23, 26]. As anticipated, viscosity declines progressively with increasing temperature. Notably, within the lower shear-rate region (130-240 s^{-1}), the system exhibits an unexpected rise in viscosity at all tested temperatures, indicating molecular rearrangements characteristic of shear-thickening behavior. Beyond shear rates exceeding 240 s^{-1}, the DES transitions to a Newtonian flow regime.

Generally, the viscosity of the DES is influenced by the characteristics of the hydrogen bond donor (HBD) and hydrogen bond acceptor (HBA) [27] while moisture content and temperature also play important roles [28]. Notably, lower viscosity of DESs is advantageous for the effective pretreatment of lignocellulosic biomass [29, 30].

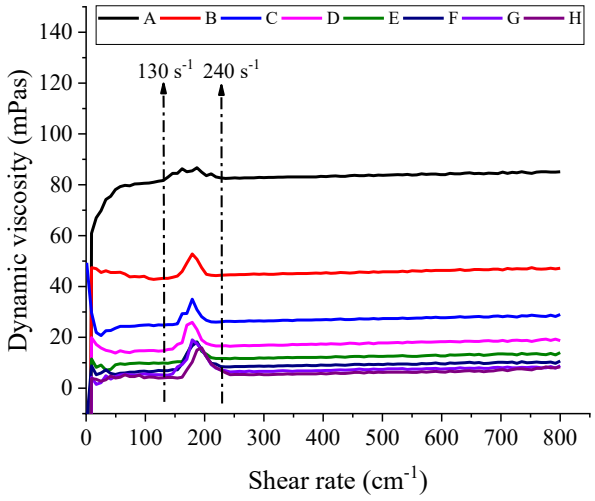


Fig. 5 Dynamic viscosities of *ChCl-LA* at variable shear rates (1 to 800 s^{-1}) and temperatures (A = 25 ºC, B = 35 ºC, C = 45 ºC, D= 55 ºC, E = 65 ºC, F = 75 ºC, G = 85 ºC and H = 95 ºC)

The thermal characteristics of *ChCl-LA* DES system (Fig. 6) were investigated using simultaneous thermogravimetric (TGA/DTG) (Fig. 6a) and differential scanning calorimetric (DSC/DDSC) analyses (Fig. 6b). The TGA curve exhibited a three-step mass loss profile of hydrogen-bonded DES system, reflecting the complex interplay between ionic interactions and component volatility. TGA/DTG curves align well with the events identified in the DSC/DDSC profiles. The initial weight loss of 4.6% up to 120 ºC is attributed to moisture evaporation from the DES system. The second stage (120-215 ºC) involves the evaporation and potential degradation of LA (around 122 ºC), accounting for a major DTG peak and a corresponding endothermic transition. 50% weight loss occurs at around 260 ºC. *ChCl*, being more thermally stable, undergoes degradation at higher temperatures, marked by two distinct peaks at the temperature range 290 to 320 ºC. After this, the TGA curve stabilizes, forming a residual mass of 4.4%.

The DSC profile revealed an endothermic event at temperature range 70-90 °C, attributed to the reorganization of hydrogen bonding in the eutectic mixture. DSC/DDSC analysis also reveal three distinct endothermic events at the temperature ranges of 105-125 ºC (T_{max} ~125 ºC), 125-220 ºC (T_{max} ~215 ºC), and 290-320 ºC (T_{max} ~305 ºC). These thermal events correspond to the

evaporation of moisture and other volatiles, the evaporation (and potential decomposition) of LA, and thermal degradation of *ChCl*, respectively.

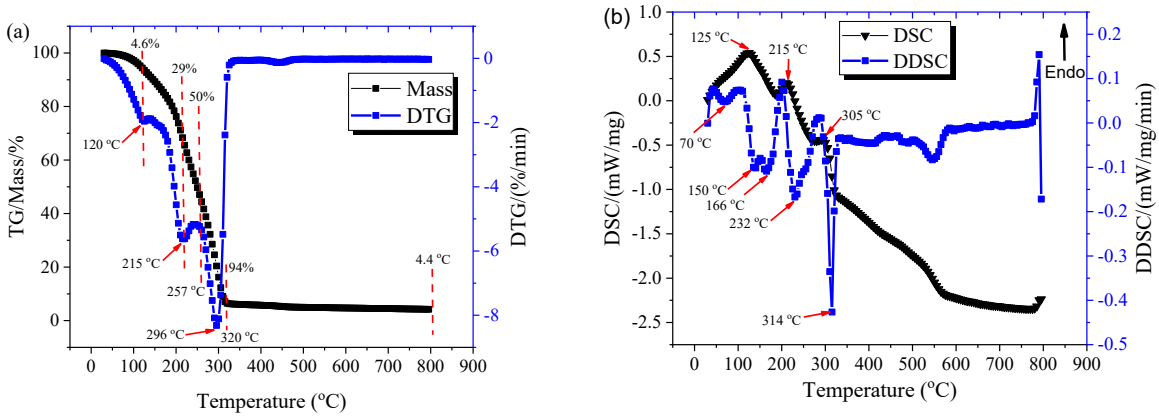


Fig. 6 Simultaneous thermal analysis of *ChCl-LA* DES system, (a) TGA and DTG curves and (b) DSC and DDSC curves

The integrated physicochemical properties of the *ChCl-LA* system, specifically its low pH, reduced dynamic viscosity at shear rates exceeding 240 s^{-1}, and robust thermal stability [31], collectively demonstrate its suitability for the efficient pretreatment of lignocellulosic biomass at <100 °C operating temperatures.

3.2 Effects of extractives and PA treatment on the isolation of DES-lignin

The efficiency of lignin isolation from SCB is strongly governed by the removal of extractives and the application of dilute PA pretreatment, as evidenced by the compositional data (SI Table S1) and fractionation results (Table 3).

Native SCB exhibits a highly recalcitrant architecture arising from covalent and noncovalent interactions within LCCs, which hinder solvent accessibility. Dilute PA pretreatment facilitates the cleavage of ester and ether linkages within these LCC structures, thereby reducing matrix rigidity and enhancing subsequent solvent penetration.

Upon treatment with the *ChCl-LA* DES system, lignin recovery increased markedly from 53.00% for native SCB to 67.43% for extractives-free SCB and reached 93.55% for extractives-free PA pretreated SCB, demonstrating the synergistic effect of sequential deconstruction [16].

Table 3 Effects of extractives and PA treatment on the isolation of *DES-lignin* from SCB

Sample	*DES-lignin* (% of Klason lignin)	*DES-cellulose*/ pulp recovery (%)	Apparent α-cellulose content (%)
Native SCB	53.00	60.10	64.06
SCB (Extractive-free)	67.43	53.83	76.47
SCB (Extractive-free and PA treated)	93.55	45.36	84.10

Concurrently, the *DES-cellulose*/pulp recovery decreased from 60.10 to 45.36%, indicating substantial removal of noncellulosic components. This selective fractionation led to a progressive increase in the apparent α-cellulose content of the recovered *DES-cellulose*/pulp from 64.06 to 84.10%. The observed enrichment is primarily attributed to the preferential solubilization of lignin and residual hemicellulosic fractions, resulting in compositional concentration of cellulose. The *ChCl-LA* DES system exhibits strong hydrogen-bonding interactions with lignin aromatic and phenolic functionalities, promoting its dissolution, while the highly ordered, hydrogen-bonded crystalline domains of cellulose remain largely resistant to solvent-induced depolymerization under the applied conditions. The presence of water in the DES further moderates solvent acidity and viscosity, suppressing undesired carbohydrate degradation and contributing to cellulose preservation. It is noted that the reported α-cellulose values represent apparent contents, which may include minor alkali insoluble noncellulosic residues.

Overall, the results confirm that the integrated PA/*ChCl-LA* DES strategy enables efficient delignification while maintaining structural integrity of cellulose, achieving a favorable balance between lignin recovery and cellulose enrichment that is critical for sustainable biorefinery applications. A comparative summary of previously reported studies [16, 32, 33, 34, 35, 36, 37] on SCB fractionation by different solvent system and conditions is provided in Table 4.

Table 4 Isolation of lignin from SCB by different solvent systems and conditions

DES system	Conditions	SCB-hemicellulose (%)	SCB-cellulose/pulp (%)	SCB-lignin (%)	Reference
Sequential H_3PO_4 and KOH pretreatment	• Sample: 2% H_3PO_4 = 1:15; Heating at 160±10 °C for 2h was used to recover hemicellulose from extractive-free SB. • Sample: 4%KOH=1:15; Heating at 170±10 °C for 2h was used to recover cellulose and lignin from acid pretreated SB.	>88%	>77%	>77%	[16]
• *ChCl-Gly* • *ChCl-Urea*	• 13.12 h, LSR 23.4:1 and 160 °C • 14.04 h, LSR 17:1 and 160 °C		• 50-80	• 81.1 • 82.0	[32]
ChCl-LA DES	LSR of 1:25, temperature of 110 °C, 12 h	• Hydrothermal pretreatment: 32.57 • Alkaline pretreatment: 66.84	• 85.3 • 81.2	• 86.7 • 79.6	[33]
ChCl-OA-MA DES	Stirred continuously at 90 °C for 4h	• 75.82	• 60.88	• 71.64	[34]
ChCl-PTSA-EG DES system	-	-	High-yield high-performance pulp	• 97.94	[35]
ChCl-OA DES system with carbon dioxide, and ethanol	-	-	• 60	• 90	[36]
ChCl-AA	LSR of 15:1 (v/w) with magnetic stirring at 130 °C and 90 min	>20% Xylan	>60% Glucan	-	[37]
Sequential H_3PO_4 and *ChCl-LA* DES pretreatment	• Sample: 2% H_3PO_4 = 1:15; Heating at 160±10 °C for 2h was used to recover hemicellulose from extractive-free SCB. • Sample: *ChCl-LA* DES =1:15; Heating at 90±5 °C for 6h with magnetic stirring	>93 Hemicellulose	>45 *DES-cellulose/pulp* from dried SCB (~84% *α-cellulose preserved*)	>93 *DES-lignin*	Present work

Notes: Gly: Glycolic acid; OA: Oxalic acid; MA= Melonic acid; PTSA: Paratoluenesulfonic acid; EG=Ethylene glycol; AA= Acetic acid

3.3 Examination of physicochemical characteristics of DES-lignin and DES-cellulose

Elemental analysis and empirical formula of DES-lignin

Elemental composition of *DES-lignin* was determined by an elemental analyzer and presented in Table 5. Elemental analysis of *DES-lignin* provided C = 56.33%, H = 5.46%, O = 38.21% and trace N (0.07%) with no detectable sulfur. The methoxyl content was 16.81%. These values correspond to atomic ratios H/C = 1.16 and O/C = 0.51 and are consistent with an aromatic biopolymer bearing abundant oxygenated functionalities.

Table 5 Elemental analysis and empirical formula of *DES-lignin* (trace amount of nitrogen was present in the samples and not considered for empirical formula determination)

Sample	%C	%H	%N	%S	%O	%OCH_3	Empirical formula
DES-lignin	56.33	5.458	0.07	-	38.21	16.81	$C_9H_{8.28}O_4(OCH_3)_{1.17}$

From the measured composition we derived an empirical repeat unit of $C_9H_{8.28}O_4(OCH_3)_{1.17}$, indicating 1.0 to 1.2 methoxyl groups per C9 unit and supporting a mixed guaiacyl-syringyl structure. The empirical formula is similar to the previously reported formula of Sugarcane bagasse alkali-lignin [16, 38].

Particle size analysis and surface morphology of DES-lignin

The particle size and distribution of *DES-lignin* were determined using dynamic light scattering (DLS). The results revealed that the *DES-lignin* exhibited a z-average particle size of 63.3 ± 18.3 nm with a dispersity (D) value of 0.158 (Fig. 7). The relatively low dispersity value indicates a narrow size distribution, suggesting that the majority of *DES-lignin* particles possess a uniform size [39].

The surface morphology of the *DES-lignin* was also examined by SEM, and the corresponding particle size distribution is presented in Fig. 8.

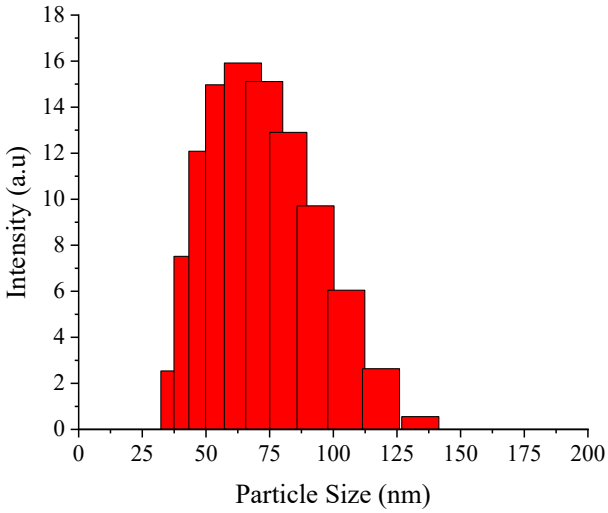


Fig. 7 Particle size analysis of *DES-lignin* by dynamic light scattering technique

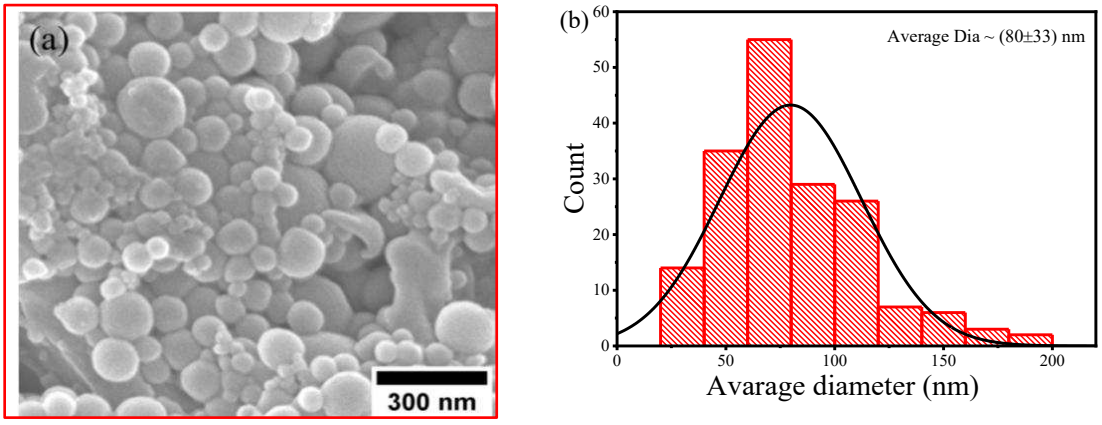


Fig. 8 SEM analysis of *DES-lignin*, (a) micrograph at 100K magnification (scale bar was set at 300 nm) and (b) Particle size distributions

Conventionally, ball-milled lignin exhibits irregular and highly heterogeneous particle shapes, characterized by angular edges and broad size distributions resulting from mechanical shearing rather than molecular self-assembly [39,41]. In contrast, the SEM micrograph of the *DES-lignin* displays uniformly dispersed, near-spherical morphology, confirming the successful formation of *DES-lignin* nanoparticles. The nanoscale spherical morphology enhances surface area and dispersibility, rendering *DES-lignin* particularly attractive for nanocomposite formation, emulsification, and functional material applications.

Analysis of functional groups, overtones and combination bands of DES-lignin

Fourier transform-Mid and Near Infrared (FT-MIR-NIR) spectroscopic analysis offers valuable insights into fundamental, overtone and combination bands generated by the lignin macromolecules [42, 43, 44, 45]. The FT-MIR spectrum of *DES-lignin* is presented in Fig. 9a**,** with corresponding absorption data detailed in SI Table S2 and the FT-NIR spectrum is presented in Fig. 9b**,** with corresponding absorption data detailed in SI Table S3**.**

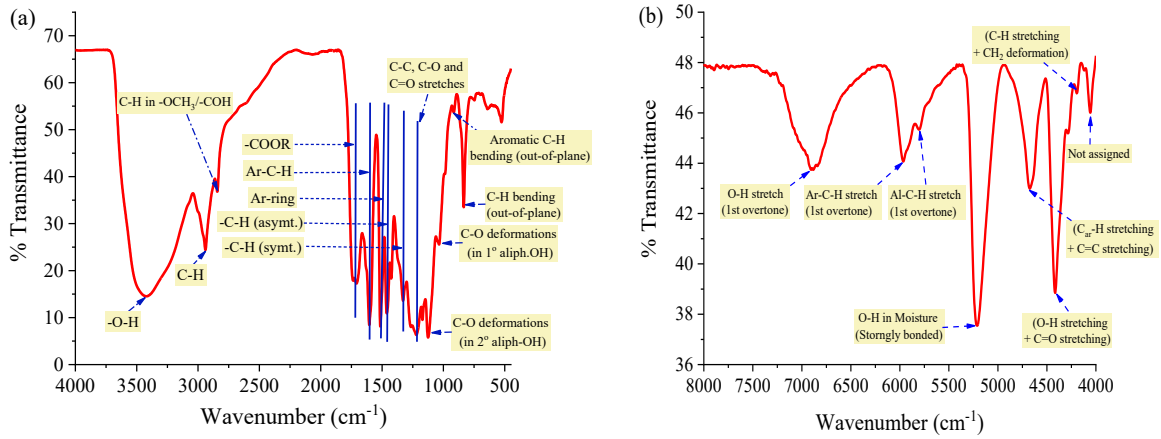


Fig. 9 FT-MIR-NIR spectra of *DES-lignin*, (a) FT-MIR spectrum and (b) FT-NIR spectrum

The FT-MIR spectra of *DES-lignin* showed a broad band around 3421 cm^{-1} represents hydrogen-bonded O-H stretching from alcoholic and phenolic groups. Aliphatic C-H asymmetric and symmetric stretching vibrations appeared at 2943 and 2840 cm^{-1}, respectively, with the latter linked to methoxyl groups. Ester-related peaks at 1709 and 1735 cm^{-1} suggest the presence of conjugated/aromatic esters. Aromatic C-H skeletal vibrations were observed at 1604 and 1514 cm^{-1}, while the peak at 1430 cm^{-1} is due to aliphatic C-H deformation. Below 1430 cm^{-1}, spectral interpretation becomes complex due to overlapping aromatic and C-H deformation modes. Peaks at 1365 and 1330 cm^{-1} are assigned to methoxyl C-H bending and phenolic OH bending, respectively. Guaiacyl-type lignin exhibits bands at 1270 cm^{-1}, and G-S type at 1275 cm^{-1}, related to ring breathing and C-O stretching. All samples showed a band near 1222 cm^{-1}, possibly from C-C, C-O, and C=O stretches. Weak bands at ~1150 cm^{-1}correspond to C-H in-plane deformations of G units, while a peak at 1121 cm^{-1} is typical of S-type lignin. The 1030 cm^{-1} band is due to aliphatic C-H and C-O stretching in primary alcohols. Absorption at 915 cm^{-1}

is linked to aromatic C-H out-of-plane deformations. Peaks near 834 cm^{-1} reflect C-H bending in S-type rings and various substituted aromatic structures [43].

The FT-NIR spectrum displays numerous overlapping, broad, and low-intensity bands, mainly arising from overtone and combination modes of C-H and O-H functional groups, making interpretation challenging. Previous studies have assigned these bands to various biomass components, such as cellulose, hemicellulose, lignin, and extractives [44, 45].

A dominant and broad absorption band around 6872 cm^{-1} corresponds to the first overtone of phenolic O-H groups involved in hydrogen bonding. A shoulder at ~5896 cm^{-1} represents the first overtone of aliphatic C-H, while a band at 5982 cm^{-1} relates to aromatic C-H overtones. Strong, sharp bands between 5204-5208 cm^{-1} indicate a combination of O-H stretching and deformation, reflecting moisture absorption [45].

Aromatic C-H and C=C combination bands appear as broad features near 4676 cm^{-1}, and a sharp band at 4418 cm^{-1} is assigned to C=O and O-H combination modes. These spectral features are consistent across *DES-lignin* and milled wood lignin from spruce and aspen, with minimal variation in peak positions [44].

Analysis of structural features and linkages through NMR analysis of DES-lignin

^{1}H, ^{13}C and ^{1}H-^{13}C HSQC-NMR spectra of *DES-lignin* are shown in Fig. 10**.** The assignments of the peaks are given in SI Table S4, SI Table S5 and SI Table S6, respectively.

The ^{1}H-NMR spectrum of *DES-lignin* revealed three distinct types of aromatic protons corresponding to guaiacyl (δ 7.2-8.0 ppm), syringyl (δ 6.7-7.1 ppm), and p-hydroxyphenyl (δ 6.2-6.7 ppm) structural units. A characteristic resonance near δ10 ppm was attributed to protons adjacent to aldehyde groups. Signals observed at δ 2.2-2.4 ppm and δ 1.6-2.2 ppm were assigned to phenolic and aliphatic ester protons, respectively, while methoxy protons resonated within δ 3.3-4.0 ppm. The hydroxyl (-OH) proton signals were poorly resolved due to overlap with side-chain protons, therefore, acetylation is often employed to improve spectral resolution. Additionally, signals at δ 5.459, 4.9, and 4.209 ppm were assigned to H_{α}, H_{β}, and H_{γ} protons in β-O-4 linkages, respectively [46, 47].

The ^{13}C-NMR spectrum of *DES-lignin* exhibits characteristic signals at δC 174.51, 166.82, and 160.40 ppm, indicative of extensive esterification, most likely arising from DES-mediated lactylation [48]. The aromatic region (δC 155-105 ppm) displays a well-defined syringyl (S),

guaiacyl (G), and p-hydroxyphenyl (H) distribution, typical of lignin derived from herbaceous feedstocks [49]. A strong methoxyl resonance at δC 56.20 ppm further supports the predominance of G and S units, reflecting a low proportion of H units. Peaks observed in the δC 31.78-14.36 ppm range correspond to acetyl/lactyl -CH_3 groups, suggesting esterification at the γ-OH positions of the lignin side chains. The ^{13}C-NMR data confirm that *DES-lignin* underwent effective extraction accompanied by partial chemical modification, featuring enhanced aliphatic carbonyl signals, preserved side-chain ester linkages, and coumaric acid-derived moieties. A comprehensive structural characterization revealed both lactic acid and choline can covalently incorporate into the lignin matrix when DES pulping is conducted at 120 °C for 6h [48]. However, at 95 ± 5 °C for 6h treatment with *ChCl-LA* DES system, only a negligible amount of nitrogen was detected in the elemental analysis of *DES-lignin* in this work, indicating that choline does not participate in covalent incorporation under mild condition. In contrast, lactic acid still modifies the lignin structure at this temperature through DES-mediated lactylation (Fig. 11). These spectral characteristics are consistent with previously reported *DES-lignin* from SCB and related biomass sources [50, 51].

In the case of *DES-lignin*, the recorded ^{1}H-^{13}C HSQC spectrum revealed a wide range of cross-peaks, which have been tentatively assigned to distinct interunit linkages, functional groups, and aromatic units (SI Table S6). These cross-peaks are distributed primarily across two spectral domains: the aliphatic region (δC/δH 90-50/6.0-2.5 ppm) and the aromatic region (δC/δH 160-90/8.0-6.0 ppm), each offering critical insights into the preservation and transformation of lignin structures during DES pretreatment.

In the aliphatic region, the β-5′ phenylcoumaran (B) substructure was identified by its β-position signal at δC/δH 53.6/3.47 ppm and the corresponding γ-position at 62.6/3.68 ppm. A prominent methoxyl (-OCH_3) signal, common to syringyl and guaiacyl units, was observed at 55.6/3.73 ppm. The β-O-4′ aryl ether linkages, the most abundant native lignin linkage, showed γ-position cross-peaks at 59.4/3.40 and 3.72 ppm (A_γ), and α-position signals at 71.8/4.87 ppm (A_α/A'_α).

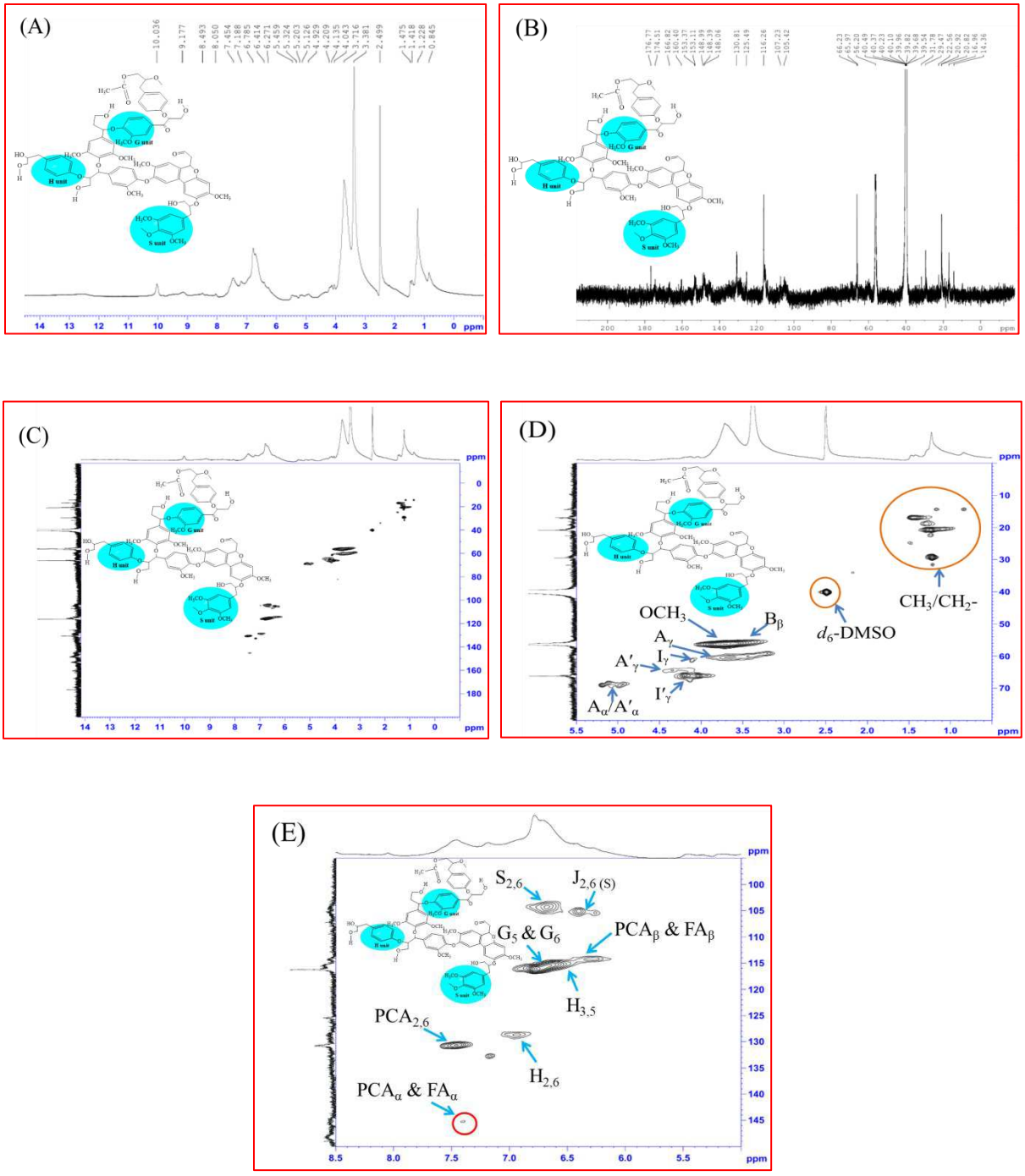


Fig. 10 ^{1}H, ^{13}C-NMR and ^{1}H-^{13}C HSQC spectra of *DES-lignin* in *d*$_6$-DMSO solution (A) ^{1}H-NMR spectrum; (B) ^{13}C-NMR spectrum; (C) ^{1}H-^{13}C HSQC spectrum (δC/δH 0-180/0-14 ppm); (D) ^{1}H-^{13}C HSQC spectrum (δC/δH 0-90/0-5.5 ppm) and (E) ^{1}H-^{13}C HSQC spectrum (δC/δH 90-180/5.5-14 ppm)

The γ-acylated variant of β-O-4′ substructures (A′$_\gamma$) appeared at 62.7/3.83-4.30 ppm, suggesting esterification at the γ-position. Cinnamyl alcohol end-groups (I) produced a signal at 61.3/4.09 ppm (I$_\gamma$), while their γ-acylated forms (I′) were assigned to peaks at 64.0/4.79 ppm (I′$_\gamma$) and 132.9/6.60 ppm (I′$_\alpha$). The β-β′ resinol (C) structure was confirmed by cross-peaks at 71.0/3.83 and 4.19 ppm (C$_\gamma$).

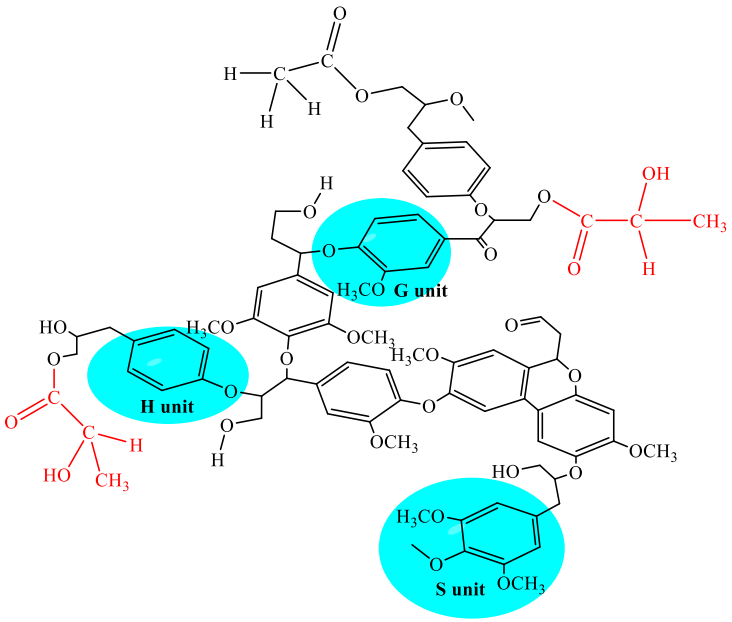


Fig. 11 *ChCl-LA* mediated lactylation of aliphatic/phenolic hydroxyl groups in *DES-lignin* (Lactyl groups are shown in red color)

The aromatic region was similarly rich in informative peaks. Etherified syringyl (S) units were clearly visible at 103.8/6.69 ppm (S$_{2,6}$), while cinnamaldehyde-type end-groups within the syringyl unit (J) showed a signal at 106.8/7.06 ppm. Signals associated with guaiacyl (G) units were resolved at 114.9/6.72 and 6.94 ppm for G$_5$, and at 118.7/6.77 ppm for G$_6$. The p-hydroxyphenyl (H) units exhibited characteristic signals at 114.5/6.62 ppm for H$_{3,5}$ and at 128.0/7.23 ppm for H$_{2,6}$. p-Coumarate (PCA) and ferulate (FA) units were identified by cross-peaks at 113.5/6.27 ppm (β-position), 144.4/7.41 ppm (α-position), 115.5/6.77 ppm (C$_{3,5}$/H$_{3,5}$), and 130.0/7.46 ppm (C$_{2,6}$/H$_{2,6}$).

Altogether, the HSQC-NMR analysis confirms that DES pretreatment preserves a diverse array of native and derivatized lignin features. The preservation of these structural motifs underscores the effectiveness of the sequential PA/*ChCl-LA* DES pretreatment in isolating lignin suitable for downstream valorization.

Assessment of thermal behaviors of DES-lignin

The thermal stability and decomposition profile of *DES-lignin* were investigated by simultaneous thermal analysis, i.e., thermogravimetric analysis (TGA/DTG) and differential scanning calorimetry (DSC/DDSC) (Fig. 12). The combined thermal data reveal multistage degradation behavior consistent with lignin macromolecules that have undergone DES-mediated extraction and partial esterification.

TGA shows an initial mass loss of <1% with an onset below 120 °C and a local DTG feature near 103 to 110 °C, which we attribute primarily to moisture desorption and the removal of residual, low-molecular-weight organics (Fig. 12a). A second mass-loss region, spanning approximately 120 to 260 °C with a DTG shoulder near 260 °C, likely corresponds to the volatilization and thermal decomposition of loosely bound esterified fragments and residual solvents. The major decomposition step occurs between 220 to 400 °C with two pronounced DTG maxima centered at around 262 °C and 365 °C. We assign the lower T_{max} (around 262 °C) to the scission of labile ether linkages (e.g., β-O-4 aryl ethers) and side-chain degradation, while the higher T_{max} (around 365 °C) reflects the breakdown of more condensed aromatic structures and cross-linked domains. At 800 °C the residual mass, i.e. char yield is around 42%, indicating substantial aromatic carbon retention and a high degree of structural condensation [52, 53].

DSC analysis (Fig. 12b) corroborates the TGA findings. A broad endothermic feature located at 140 to 160 °C is observed and interpreted as a thermal softening/glass transition region (T_g) for *DES-lignin,* the broadness is consistent with the heterogeneous, polydisperse nature of lignin and the presence of acylated side chains identified by ^{13}C-NMR and HSQC-NMR analyses. Subsequent exothermic features between 200 to 280 °C and 310 to 360 °C are consistent with the onset of condensation reactions and major bond scission events associated with aromatic decomposition, respectively. The presence of γ-acetylated β-O-4 signals in HSQC-NMR and ^{13}C-NMR is likely responsible for the slight shift of the β-O-4 scission T_{max} to the lower end of reported ranges, as the esterification generally decreases thermal stability of labile side-chain linkages, but increases overall char-forming propensity due to enhanced crosslinking upon heating [54, 55].

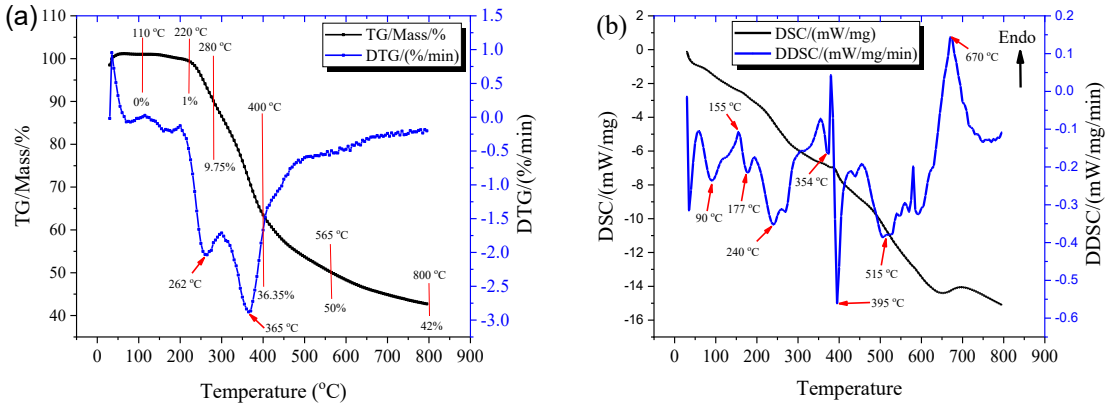


Fig. 12 Simultaneous thermal analysis of *DES-lignin*, (a) TGA-DTG and (b) DSC-DDSC thermograms of *DES-lignin* sample

Compared to Kraft and dioxane isolates, the *DES-lignin* exhibits a relatively high char yield and clearly resolved multistage degradation, consistent with preserved aromatic structures and partial chemical modification introduced during DES extraction. The high char yield (around 42%) suggests *DES-lignin* is a promising precursor for carbonaceous materials and thermally stable biocomposites.

Therefore, the combined TGA/DTG and DSC/DDSC data demonstrate that DES extraction yields a lignin fraction of high aromatic content with enhanced char-forming ability and a multistage thermal degradation. These thermal characteristics align with the structural features observed by NMR and FT-MIR-NIR and support the potential of *DES-lignin* for high-value thermally processed applications.

Intrinsic viscosity and solution behavior of DES-lignin

The intrinsic viscosity values of *DES-lignin* and related data are presented in Table 6. Intrinsic viscosity ([η]) reflects the hydrodynamic volume of solvated macromolecules and is influenced by solvent type, solute characteristics, and temperature. For a rigid, non-swelling sphere, [η] (in 100 mL/g) is expressed by the Einstein equation [55]:

$$[\eta] = 0.025\,V \qquad (4)$$

Where, V denotes the solute volume. In the case of a porous, solvent-swollen macromolecule, V corresponds to the swollen volume per unit solute weight; hence, [η] increases with molecular expansion in the solvent. Lower [η] values for a given molecular weight indicate compact

molecular conformations. Previous studies reported comparatively low intrinsic viscosities for various lignin preparations, confirming their compact nature in solution [56, 57]. For instance, [η] values of 4.1-10.7 mL/g for dioxane lignin fractions from *Serratula coronata* L. consistent with data for *Betula pendula* lignin [56]. Goring reported [η] values of 10 and 8 mL/g for sodium lignosulfonate and spruce dioxane lignin [55], respectively, while Kraft lignin exhibited 6.9-8.1 mL/g in dimethylformamide [58]. These values significantly lower than those of conventional polymers; highlight the compact, highly cross-linked nature of lignin macromolecules in solution. *DES-lignin* also showed similar intrinsic viscosity value (8.5 mL/g) and considered as compact macromolecular structure.

Table 6 Intrinsic viscosities of *DES-lignin* in DMSO measured at 25 ºC (Dynamic viscosity of DMSO is 1.99 mPa.s at 25 ºC)

Lignin	Relative viscosity	Inherent viscosity (mL/g)	Specific viscosity	Reduced viscosity (mL/g)	Intrinsic viscosity (mL/g)
DES-lignin	1.017	8.5	1.7	8.5	8.5

X-ray diffraction analysis of DES-cellulose

X-ray diffractogram of *DES-cellulose/pulp* is given in Fig. 13 and tentative assignments of the crystalline peaks are described in SI Table S7**.**

The XRD profile of commercial cellulose displayed characteristic cellulose I reflections at 2θ = 16.2°, 23.4°, and 38.5°, corresponding to the (110), (200), and (004) crystallographic planes of the native cellulose I allomorph [59, 60]. In contrast, the sequential PA followed by *ChCl-LA* DES pretreatments resulted in the appearance of new peaks at 12.2° and 20.3°, along with a shoulder at 22.1° and a shifted high-angle band at 37.7° [61, 62]. The low-angle peak at 12.2° and the dominant peak at 20.3° are well-established signatures of cellulose II, indicating that the pretreatments disrupted the native parallel-chain cellulose I lattice and promoted antiparallel chain rearrangement during regeneration [63].

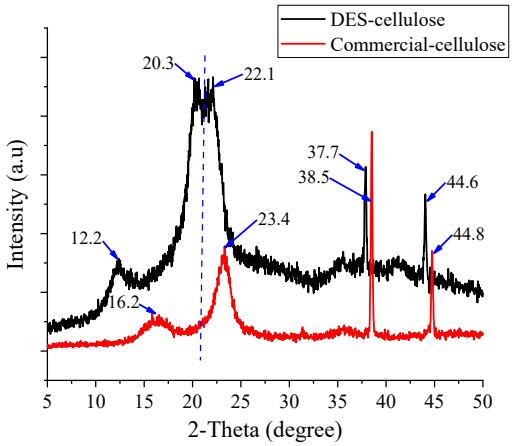


Fig. 13 X-ray diffraction analysis of commercial cellulose (2θ = 16.2°, 23.4°, and 38.5°, corresponding to the 110, 200, and 004 planes, which are characteristics of cellulose I) and *DES-cellulose (*2θ = 12.2° and 20.3°, along with a shoulder at 22.1° and a shifted high-angle peak at 37.7°, which are well-established signatures of cellulose II)

The presence of the minor peak at 22.1° suggests the coexistence of residual cellulose I crystallites or mixed polymorphic domains typical of partially transformed substrates. The shift and reduced intensity of the high-angle peak (~37.7°) further reflect lower crystallinity and decreased crystallite size, arising from extensive hydrogen-bond disruption and microfibril amorphization [64]. Collectively, these changes confirm that the pretreatment sequence induced partial conversion of cellulose I to cellulose II, accompanied by significant amorphization due to the selective removal of hemicellulose and lignin and weakening of the native hydrogen-bond network.

3.4 Plausible mechanism for synergistic sequential PA/ChCl-LA DES pretreatment

The sequential pretreatment of extractive-free lignocellulosic biomass using dilute PA followed by *ChCl-LA* DES proceeds via a synergistic chemo-physical mechanism integrating selective matrix deconstruction with solvation-driven lignin extraction (Fig. 14). Prior removal of extractives eliminates low-molecular-weight phenolics, radicals, and inorganic ions, thereby suppressing side reactions and enabling controlled fractionation.

Mechanism:

Plausible mechanism for synergistic sequential PA/*ChCl-L*A DES pretreatment on extractive-free lignocellulosic biomass is discussed below:

First step: As illustrated in Fig. 14, dilute PA selectively hydrolyzes hemicellulosic glycosidic bonds under mild, non-oxidative conditions, resulting in hemicellulose solubilization while preserving lignin structure. The moderate acidity limits benzylic carbocation formation, preventing cleavage of β-O-4 linkages and suppressing condensation. This step primarily opens the biomass matrix, increasing porosity and exposing lignin domains.

Second step: Following matrix opening, the *ChCl-LA* DES penetrates the structure and disrupts lignin-carbohydrate complexes (LCCs) through hydrogen bonding and electrostatic interactions. *LA* acts as a hydrogen bond donor and mild acid, while *ChCl* functions as a hydrogen bond acceptor and ionic stabilizer. Lignin extraction occurs predominantly via a solvation mechanism rather than extensive covalent bond cleavage, enabling recovery of structurally preserved lignin. Consequently, lignin is extracted in a structurally preserved form, with minimal alteration to its native architecture, supported by intrinsic viscosity measurement that showed similar molecular density as dioxane lignin [55]. *ChCl-LA* DES mediated lactylation in aliphatic/phenolic hydroxyl groups can occur during pretreatment.

Third step: The DES environment stabilizes solubilized lignin through extensive hydrogen bonding, while rapid dissolution limits the lifetime of reactive intermediates and suppresses condensation. The hydrogen bond rich, low dielectric medium further restricts repolymerization. Structural analyses (e.g., HSQC-NMR) confirm the preservation of β-O-4 linkages with minimal formation of condensed structures (e.g., β-5, β-β).

Forth step: Finally, the addition of water disrupts the solvation equilibrium, inducing lignin precipitation, while cellulose remains largely undissolved due to its crystalline structure. This enables efficient lignin recovery and DES recyclability.

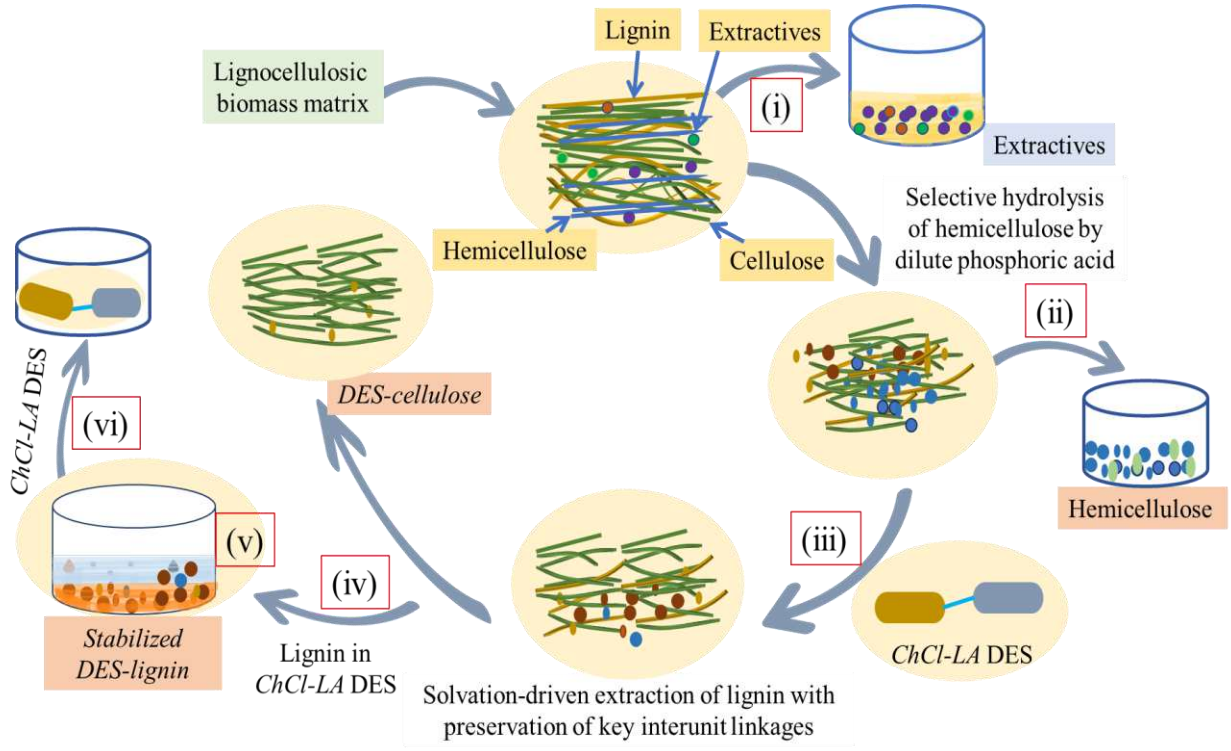


Fig. 14 Plausible mechanism for synergistic sequential PA/*ChCl-LA* DES pretreatment and fractionation of the structural components of lignocellulosic biomass. The process involves- (i) removal of extractives to eliminate reactive impurities, (ii) selective hydrolysis of hemicellulose by PA under mild, non-oxidative conditions, resulting in matrix opening and increased lignin accessibility, (iii) penetration of *ChCl-LA* DES into the pretreated biomass and disruption of lignin-carbohydrate complexes via hydrogen bonding and electrostatic interactions, (iv) solvation driven extraction of lignin with preservation of key interunit linkages (e.g., β-O-4, etc.), (v) suppression of lignin condensation due to limited carbocation formation and rapid stabilization of lignin fragments, and (vi) recovery of lignin through water induced precipitation with simultaneous recycling of the DES.

Overall, the mechanism highlights the synergistic interplay between selective acid-mediated matrix deconstruction and gentle DES-based solvation, enabling high efficiency fractionation while maintaining lignin in a near-native structural bonding states.

3.5 Prospects of the synergistic sequential PA/ChCl-LA DES Lignocellulosic Biorefinery System

It is well-known that the enzymatic hydrolysis of untreated lignocellulosic biomass is severely hindered by lignin shielding, high cellulose crystallinity, hemicellulose-lignin cross-linking, presence of extractives and, low porosity, all of which limit enzyme accessibility and promote non-productive adsorption [65-67]. Pretreatment addresses these barriers by removing or redistributing lignin, solubilizing hemicellulose, reducing cellulose crystallinity, and increasing surface area and pore volume, while also eliminating inhibitory extractives. These structural alterations substantially enhance enzyme penetration and catalytic efficiency, leading to higher sugar release and improved conversion of lignocellulosic substrates to bioethanol. An overview of the synergistic sequential PA/*ChCl-LA* DES-based lignocellulosic biorefinery model for the production of biofuels and bio-based materials (Fig. 15).

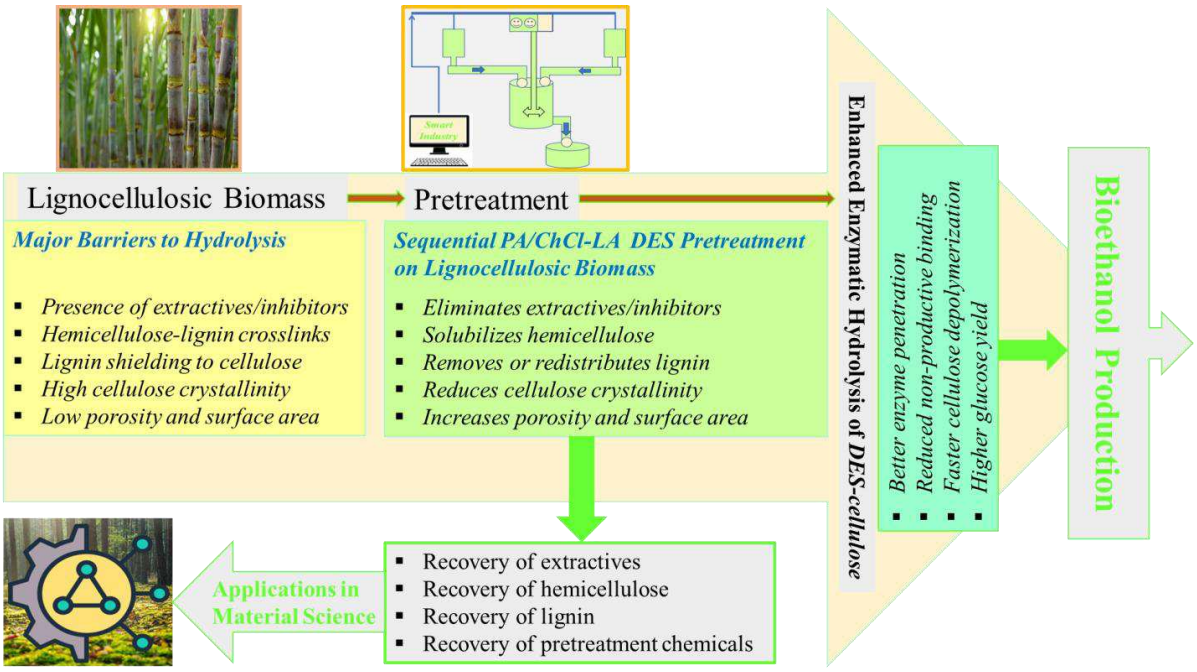


Fig. 15 An overview of the synergistic sequential PA/*ChCl-LA* DES-based lignocellulosic biorefinery model for the production of biofuels and bio-based materials

The efficient recovery of all biomass fractions and pretreatment chemicals is essential for establishing a truly circular and sustainable biorefinery. Extractives can be used as value-added antioxidants, natural surfactants, or antimicrobial agents, thereby reducing organic load in

downstream liquors. Hemicellulose, recovered as oligosaccharides or monomeric sugars in dilute phosphoric acid, serves as a versatile platform for producing materials, e.g., agrochemicals [68, 69], biofuels, xylitol, furans, and prebiotic ingredients.

DES-lignin obtained in structurally preserved or modified forms, can be valorized in high-performance materials, e.g., flame retardants [38], adsorbents [70] resins, and polymer additives, contributing significantly to the economic viability of the process. The recovered *DES-cellulose* can be used to produce nanofibrillated cellulose, bioethanol, platform chemicals (e.g., glucose, HMF, levulinic acid), etc. Simultaneously, the efficient reclamation and recycling of pretreatment chemicals, e.g., acid, alkali [16] and deep eutectic solvent components along with other solvents used, not only lowers operating cost but also minimizes environmental burdens. Together, these integrated recovery strategies ensure maximal resource utilization, reduced waste generation, and enhanced process sustainability within modern biorefinery frameworks.

Future work would prioritize the reusability of *ChCl-LA* DES system, comprehensive techno-economic and life-cycle assessment, etc. These efforts are essential for transforming this laboratory-scale concept into an industrially viable biorefinery platform.

4. Conclusion

The study provides a robust foundation for developing scalable and environmentally benign phosphoric acid and choline chloride-lactic acid deep eutectic solvent based lignocellulosic biorefinery system. The phosphoric acid stage effectively solubilized approximately 93.5% of hemicellulose from extractive-free SCB and enhanced cell wall accessibility, while the subsequent deep eutectic solvent treatment enabled the selective recovery of 93.7% lignin and over 45% (w/w) cellulose-rich pulp. Isolated lignin exhibited nanoscale dimensions (~63 nm), near spherical morphology, and well-preserved guaiacyl-syringyl-p-hydroxyphenyl (G-S-H) structures, as confirmed by FT-MIR-NIR, NMR, and thermal analyses. XRD data of recovered cellulose pulp revealed a marked shift and reduced intensity of the high-angle peak (~37.7°) reflect lower crystallinity and decreased crystallite size, arising from extensive hydrogen-bond disruption and may improve the enzymatic or catalytic accessibility. The integrated phosphoric acid and choline chloride-lactic acid deep eutectic solvent system thus offers a mild, recyclable, and scalable platform for comprehensive biomass valorization. Its high selectivity, effective component recovery, and minimal environmental footprint position this approach as a promising

candidate for next-generation lignocellulosic biorefineries. Furthermore, the nanolignin obtained through this process holds significant potential for advanced material applications such as bio-based composites, resins, and carbon precursors, aligning with the principles of circular bioeconomy and green chemistry.

Data availability

The data supporting this article have been included as part of the Supplementary Information (SI). Additional data from the study are available upon request.

Supporting Information

The supporting information encompasses: Components in Sugarcane bagasse, concise overview of the methodologies employed; FT-MIR-NIR spectral data and tentative assignments; ^{1}H and ^{13}C and HSQC-NMR spectral data and tentative assignments, XRD data and tentative assignments, etc.

Authors' contribution

Md. Rashed Hasan: Data curation, Investigation, Original draft preparation; Nigar Fatima: Data curation, Investigation, Reviewing and Editing; Sonia Akter: Data curation, Investigation; Md. Saiful Islam: Data curation, Investigation; Md. Farid Ahmed: Data curation, Investigation; Mohammad Majedul Haque: Data curation, Investigation; S. M. Asaduzzaman Sujan: Data curation, Investigation, Methodology; Swapan Kumer Ray: Conceptualization, Methodology, Supervision, Reviewing and Editing

Acknowledgements

This work was supported by the Bangladesh Council of Scientific and Industrial Research (BCSIR) under its Regular R&D Program and did not receive any additional or external specific funding.

References

[1] Bozell, J. J., & Petersen, G. R. (2010). Technology development for the production of biobased products from biorefinery carbohydrates- the US Department of Energy's "Top 10" revisited. *Green chemistry*, *12*(4), 539-554. https://doi.org/10.1039/B922014C

[2] Tuck, C. O., Pérez, E., Horváth, I. T., Sheldon, R. A., & Poliakoff, M. (2012). Valorization of biomass: deriving more value from waste. *Science*, *337*(6095), 695-699. https://doi.org/10.1126/science.1218930

[3] Pahlavanlu, P., Klain, A., Lessard, J. M., Blair, J., Gagnon, B., (2022). How Can Biomass Supply for Bioenergy Deliver Multiple Benefits and Contribute to Sustainable Development Goals. Report from Joint IEA Bioenergy and GBEP Workshop held online on 15-16 June 2021.www.ieabioenergy.com/wp-content/uploads/2022/03/IEA-Bioenergy_Report-Biomass_Supply-SDGs-Final.pdf (Last accessed in 12 April, 2026)

[4] El-Araby, R. (2024). Biofuel production: exploring renewable energy solutions for a greener future. Biotechnology for Biofuels and Bioproducts, 17(1), 129. https://doi.org/10.1186/s13068-024-02571-9

[5] Cherubini, F. (2010). The biorefinery concept: Using biomass instead of oil for producing energy and chemicals. Energy conversion and management, 51(7), 1412-1421. https://doi.org/10.1016/j.enconman.2010.01.015

[6] Maity, S. K. (2015). Opportunities, recent trends and challenges of integrated biorefinery: Part II. Renewable and Sustainable Energy Reviews, 43, 1446-1466. https://doi.org/10.1016/j.rser.2014.08.075

[7] Joshi, M., & Manjare, S. (2024). Chemical approaches for the biomass valorisation: a comprehensive review of pretreatment strategies. Environmental Science and Pollution Research, 31(36), 48928-48954. https://doi.org/10.1007/s11356-024-34473-6

[8] Jönsson, L. J., & Martín, C. (2016). Pretreatment of lignocellulose: formation of inhibitory by-products and strategies for minimizing their effects. Bioresource technology, 199, 103-112. https://doi.org/10.1016/j.biortech.2015.10.009

[9] Chandra, R. P., Bura, R., Mabee, W. E., Berlin, D. A., Pan, X., & Saddler, J. N. (2007). Substrate pretreatment: the key to effective enzymatic hydrolysis of lignocellulosics?. Biofuels, 67-93. https://doi.org/10.1007/10_2007_064

[10] Ragauskas, A. J., Beckham, G. T., Biddy, M. J., Chandra, R., Chen, F., Davis, M. F., Davison, B. H., Dixon, R. A., Gilna, P., Keller, M., Langan, P., Naskar, A. K., Saddler, J. N., Tschaplinski, T. J., Tuskan, G. A., Wyman, C. E. (2014). Lignin valorization: improving lignin processing in the biorefinery. science, 344(6185), 1246843. https://doi.org/10.1126/science.1246843

[11] Argyropoulos, D. D., Crestini, C., Dahlstrand, C., Furusjö, E., Gioia, C., Jedvert, K., ... & Wimby, M. (2023). Kraft lignin: a valuable, sustainable resource, opportunities and challenges. *ChemSusChem*, *16*(23), e202300492. https://doi.org/10.1002/cssc.202300492

[12] Kai, D., Tan, M. J., Chee, P. L., Chua, Y. K., Yap, Y. L., & Loh, X. J. (2016). Towards lignin-based functional materials in a sustainable world. *Green Chemistry*, *18*(5), 1175-1200. https://doi.org/10.1039/C5GC02616D

[13] Beisl, S., Miltner, A. and Friedl, A., (2017). Lignin from micro-to nanosize: production methods. *International journal of molecular sciences*, *18*(6), p.1244. https://doi.org/10.3390/ijms18061244

[14] Duarah, P., Haldar, D. and Purkait, M.K., (2020). Technological advancement in the synthesis and applications of lignin-based nanoparticles derived from agro-industrial waste residues: A review. *International Journal of Biological Macromolecules*, *163*, pp.1828-1843. https://doi.org/10.1016/j.ijbiomac.2020.09.076

[15] Iravani, S. and Varma, R.S., (2020). Greener synthesis of lignin nanoparticles and their applications. *Green Chemistry*, *22*(3), pp.612-636. https://doi.org/10.1039/C9GC02835H

[16] Ray, S. K., Bhuiyan, R. H., Muslim, T., & Ehsan, M. Q. (2024). Development of a material-driven phase III lignocellulosic feedstock biorefinery system. ACS Sustainable Resource Management, 1(9), 1994-2013. https://doi.org/10.1021/acssusresmgt.4c00168

[17] du Pasquier, J., Paës, G., & Perré, P. (2023). Principal factors affecting the yield of dilute acid pretreatment of lignocellulosic biomass: a critical review. Bioresource Technology, 369, 128439. https://doi.org/10.1016/j.biortech.2022.128439

[18] de Vasconcelos, S. M., Santos, A. M. P., Rocha, G. J. M., & Souto-Maior, A. M. (2013). Diluted phosphoric acid pretreatment for production of fermentable sugars in a sugarcane-based biorefinery. Bioresource technology, 135, 46-52. https://doi.org/10.1016/j.biortech.2012.10.083

[19] Kim, J. S., Lee, Y. Y., & Kim, T. H. (2016). A review on alkaline pretreatment technology for bioconversion of lignocellulosic biomass. Bioresource technology, 199, 42-48. doi: https://doi.org/10.1016/j.biortech.2015.08.085

[20] Duarte, L. C., Sampaio, B., & Carvalheiro, F. (2024). Organosolv Pretreatment of Lignocellulosic Biomass. In Handbook of Biorefinery Research and Technology (pp. 1-28). Springer, Dordrecht. https://doi.org/10.1007/978-94-007-6308-1_81

[21] Zhang, J., Zou, D., Singh, S., & Cheng, G. (2021). Recent developments in ionic liquid pretreatment of lignocellulosic biomass for enhanced bioconversion. Sustainable Energy & Fuels, 5(6), 1655-1667. https://doi.org/10.1039/D0SE01802C

[22] Li, P., Yang, C., Jiang, Z., Jin, Y., & Wu, W. (2023). Lignocellulose pretreatment by deep eutectic solvents and related technologies: A review. Journal of Bioresources and Bioproducts, 8(1), 33-44. doi.org/10.1016/j.jobab.2022.11.004

[23] Sazali, A. L., AlMasoud, N., Amran, S. K., Alomar, T. S., Pa'ee, K. F., El-Bahy, Z. M., ... & Chuah, L. F. (2023). Physicochemical and thermal characteristics of choline chloride-based deep eutectic solvents. Chemosphere, 338, 139485 https://doi.org/10.1016/j.chemosphere.2023.139485

[24] Pires, I. V., da Cruz Rodrigues, A. M., de Souza Pinheiro, W. B., Cardoso, L. N., Saldaña, M. D., & da Silva, L. H. M. (2025). Physicochemical properties, antioxidant potential, and spectroscopic investigation of choline chloride-lactic acid NADES: Effects of molar ratio and added water. Journal of Molecular Liquids, 128414. https://doi.org/10.1111/1541-4337.70057

[25] Wei, Q., Shi, C., Wang, D., Yang, J., Shi, Z., Wen, J. L., & Yang, H. Y. (2025). Metal chloride mediated choline chloride-lactic acid deep eutectic solvent pretreatment of bamboo for improved cellulose saccharification and lignin recovery. International Journal of Biological Macromolecules, 305, 141107. https://doi.org/10.1016/j.ijbiomac.2025.141107

[26] Alcalde, R., Gutiérrez, A., Atilhan, M., & Aparicio, S. (2019). An experimental and theoretical investigation of the physicochemical properties on choline chloride–Lactic acid based natural deep eutectic solvent (NADES). Journal of Molecular Liquids, 290, 110916. https://doi.org/10.1016/J.MOLLIQ.2019.110916

[27] Elhamarnah, Y., AlRasheedi, M., AlMarri, W., AlBadr, A., AlMalki, A., Mohamed, N., ... & Qiblawey, H. (2022). An experimental investigation on the thermo-rheological behaviors of lactic acid-based natural deep eutectic solvents. Materials, 15(11), 4027 https://doi.org/10.3390/ma15114027

[28] Zhang, X., Liu, A., Li, X., Xu, W., Duan, X., Shi, J., & Li, X. (2025). Research progress of deep eutectic solvents in lignocellulosic biomass pretreatment. Cellulose, 1-14. https://doi.org/10.1007/s10570-025-06553-4

[29] Škulcová, A., & Jablonský, M. (2018). Properties and thermal behavior of deep eutectic solvents based lactic acid.

[30] Shen, X. J., Wen, J. L., Mei, Q. Q., Chen, X., Sun, D., Yuan, T. Q., & Sun, R. C. (2019). Facile fractionation of lignocelluloses by biomass-derived deep eutectic solvent (DES) pretreatment for cellulose enzymatic hydrolysis and lignin valorization. Green chemistry, 21(2), 275-283. https://doi.org/10.1039/C8GC03064B

[31] Liu, S., Yu, D., Chen, Y., Shi, R., Zhou, F., & Mu, T. (2022). High-resolution thermogravimetric analysis is required for evaluating the thermal stability of deep eutectic solvents. Industrial & Engineering Chemistry Research, 61(38), 14347-14354. https://doi.org/10.1021/acs.iecr.2c02240

[32] Varilla-Mazaba, A., Raggazo-Sánchez, J. A., Calderón-Santoyo, M., Gómez-Rodríguez, J., & Aguilar-Uscanga, M. G. (2022). Optimization of lignin extraction by response surface methodology from sugarcane bagasse using deep eutectic solvents (DES). Industrial Crops and Products, 184, 115040. https://doi.org/10.1016/j.indcrop.2022.115040

[33] Wang, N., Xu, B., Wang, X., Lang, J., & Zhang, H. (2022). Chemical and structural elucidation of lignin and cellulose isolated using DES from bagasse based on alkaline and hydrothermal pretreatment. Polymers, 14(14), 2756. https://doi.org/10.3390/polym14142756

[34] Yang, Y., Zhao, L., Ren, J., & He, B. (2022). Effect of ternary deep eutectic solvents on bagasse cellulose and lignin structure in low-temperature pretreatment. Processes, 10(4), 778. https://doi.org/10.3390/pr10040778

[35] Zhu, Y., Li, L., Hou, Y., Xu, C., Hu, G., Man, Y., ... & Xiong, Q. (2024). Investigation into the characteristics of bagasse processed with 3C-DES and the production of chemimechanical pulp for pulp molded. Journal of Cleaner Production, 447, 141652. https://doi.org/10.1021/acssuschemeng.6b00603

[36] Escobar, E. L. N., Suota, M. J., Ramos, L. P., & Corazza, M. L. (2022). Combination of green solvents for efficient sugarcane bagasse fractionation. Biomass and Bioenergy, 161, 106482. https://doi.org/10.1016/j.biombioe.2022.106482

[37] Morán-Aguilar, M. G., Costa-Trigo, I., Aguilar-Uscanga, M. G., Paz, A., & Domínguez, J. M. (2024). Development of sustainable sugarcane bagasse biorefinery using a greener deep eutectic solvent from hemicellulose-derived acids. Biomass and Bioenergy, 186, 107256. https://doi.org/10.1016/j.biombioe.2024.107256

[38] Ray, S. K., Bhuiyan, R. H., Khanam, S., Muslim, T., & Ehsan, Q. (2025). The acetobromination of alkali-lignin through a flow chemistry approach. International Journal of Biological Macromolecules, 145451. doi.org/10.1016/j.ijbiomac.2025.145451

[39] Luo, T., Wang, C., Ji, X., Yang, G., Chen, J., Janaswamy, S., & Lyu, G. (2021). Preparation and characterization of size-controlled lignin nanoparticles with deep eutectic solvents by nanoprecipitation. Molecules, 26(1), 218. https://doi.org/10.3390/molecules26010218

[40] Qu, Y., Luo, H., Li, H., & Xu, J. (2015). Comparison on structural modification of industrial lignin by wet ball milling and ionic liquid pretreatment. Biotechnology Reports, 6, 1-7. https://doi.org/10.1016/j.btre.2014.12.011

[41] Sapouna, I., van Erven, G., Heidling, E., Lawoko, M., & McKee, L. S. (2023). Impact of extraction method on the structure of lignin from ball-milled hardwood. ACS sustainable chemistry & engineering, 11(43), 15533-15543. https://doi.org/10.1021/acssuschemeng.3c02977

[42] Lin, S.Y. and Dence, C.W., Eds. (1992) Methods in Lignin Chemistry. Springer Series in Wood Science. Springer, Berlin, Heidelberg, 527-548. https://doi.org/10.1007/978-3-642-74065-7

[43] Ji, Q., Yu, X., Wu, P., Yagoub, A. E. G. A., Chen, L., Taiye, M. A., & Zhou, C. (2021). Pretreatment of sugarcane bagasse with deep eutectic solvents affect the structure and morphology of lignin. Industrial Crops and Products, 173, 114108. https://doi.org/10.1016/j.indcrop.2021.114108

[44] Schwanninger, M., Rodrigues, J. C., & Fackler, K. (2011). A review of band assignments in near infrared spectra of wood and wood components. Journal of Near Infrared Spectroscopy, 19(5), 287-308. https://doi.org/10.1255/jnirs.955

[45] Workman Jr, J., & Weyer, L. (2007). Practical guide to interpretive near-infrared spectroscopy. CRC press. https://doi.org/10.1201/9781420018318

[46] Li, S., & Lundquist, K. (2001). Analysis of hydroxyl groups in lignins by 1H NMR spectrometry. Nordic Pulp & Paper Research Journal, 16(1), 63-67. https://doi.org/10.3183/npprj-2001-16-01-p063-067

[47] Ralph, J. and Landucci, L. L. (2010). NMR of Lignins. in Lignin and Lignans; Advances in Chemistry, eds. C. Heitner, D. R. Dimmel and J. A. Schmidt, CRC Press (Taylor & Francis Group), Boca Raton, FL, 2010, pp. 137-234. https://doi.org/10.1201/EBK1574444865

[48] van Erven, G., Boerkamp, V. J., van Groenestijn, J. W., & Gosselink, R. J. (2024). Choline and lactic acid covalently incorporate into the lignin structure during deep eutectic solvent pulping. Green Chemistry, 26(12), 7101-7112. https://doi.org/10.1039/D4GC00909F

[49] Chen, C. L., & Robert, D. (1988). Characterization of lignin by 1H and 13C NMR spectroscopy. In Methods in enzymology (Vol. 161, pp. 137-174). Academic Press. https://doi.org/10.1016/0076-6879(88)61017-2

[50] Ji, Q., Yu, X., Wu, P., Yagoub, A. E. G. A., Chen, L., Taiye, M. A., & Zhou, C. (2021). Pretreatment of sugarcane bagasse with deep eutectic solvents affect the structure and morphology of lignin. Industrial Crops and Products, 173, 114108. https://doi.org/10.1016/j.indcrop.2021.114108

[51] Antoun, K., Tabib, M., Salameh, S. J., Koubaa, M., Ziegler-Devin, I., Brosse, N., & Khelfa, A. (2024). Isolation and Structural Characterization of Natural Deep Eutectic Solvent Lignin from Brewer's Spent Grains. Polymers, 16(19), 2791. https://doi.org/10.3390/polym16192791

[52] Amit, T. A., Roy, R., & Raynie, D. E. (2021). Thermal and structural characterization of two commercially available technical lignins for potential depolymerization via hydrothermal liquefaction. Current Research in Green and Sustainable Chemistry, 4, 100106. https://doi.org/10.1016/j.crgsc.2021.100106

[53] Chen, Z.; Bai, X.L.; Lusi, A.; Zhang, H.W.; Wan, C.X. Insights into structural changes of lignin toward tailored properties during deep Eutectic solvent pretreatment. ACS Sustain. Chem. Eng. 2020, 8, 9783–9793. https://doi.org/10.1021/acssuschemeng.0c01361

[54] Yang, Y., Zhao, L., Ren, J., & He, B. (2022). Effect of ternary deep eutectic solvents on bagasse cellulose and lignin structure in low-temperature pretreatment. Processes, 10(4), 778. https://doi.org/10.3390/pr10040778

[55] Goring, D. A. I. (1962). The physical chemistry of lignin. Pure and applied chemistry, 5(1-2), 233-310. doi:10.1351/pac196205010233

[56] Karmanov, A. P., Kocheva, L. S., Belyi, V. A., & Volodin, V. V. (2019). Transport Properties and Sizes of Lignin Macromolecules in Solution. Polymer Science, Series A, 61(1), 53-60. https://doi.org/10.1134/S0965545X1901005X

[57] Kocheva, L. S., Karmanov, A. P., & Karmanova, Y. A. (2014). Evaluation of the scaling parameters of lignin macromolecules. Russian Chemical Bulletin, 63(9), 2036-2039. https://doi.org/10.1007/s11172-014-0696-2

[58] Dong, D., & Fricke, A. L. (1995). Intrinsic viscosity and the molecular weight of kraft lignin. Polymer, 36(10), 2075-2078. https://doi.org/10.1016/0032-3861(95)91455-G

[59] French, A. D. (2014). Idealized powder diffraction patterns for cellulose polymorphs. Cellulose, 21(2), 885-896. https://doi.org/10.1007/s10570-013-0030-4

[60] Gong, J., Li, J., Xu, J., Xiang, Z., & Mo, L. (2017). Research on cellulose nanocrystals produced from cellulose sources with various polymorphs. RSC advances, 7(53), 33486-33493. https://doi.org/10.1039/C7RA06222B

[61] Rasheed, H. A., Adeleke, A. A., Nzerem, P., Olosho, A. I., Ogedengbe, T. S., & Jesuloluwa, S. (2024). Isolation, characterization and response surface method optimization of cellulose from hybridized agricultural wastes. *Scientific Reports*, *14*(1), 14310. https://doi.org/10.1038/s41598-024-65229-4

[62] Langan, P., Nishiyama, Y., & Chanzy, H. (1999). A revised structure and hydrogen-bonding system in cellulose II from a neutron fiber diffraction analysis. Journal of the American Chemical Society, 121(43), 9940-9946. https://doi.org/10.1021/ja9916254

[63] Isogai, A., Atalla, R.H. Dissolution of Cellulose in Aqueous NaOH Solutions. *Cellulose* **5**, 309–319 (1998). https://doi.org/10.1023/A:1009272632367

[64] Li, M., Zhang, Q., Chen, C., Wang, S., & Min, D. (2019). Lignin interaction with cellulase during enzymatic hydrolysis. Pap. Biomater, 4(4), 15-30. https://doi.org/10.26599/PBM.2019.9260026

[65] Wang, Z., Zhu, J. Y., Fu, Y., Qin, M., Shao, Z., Jiang, J., & Yang, F. (2013). Lignosulfonate-mediated cellulase adsorption: enhanced enzymatic saccharification of lignocellulose through weakening nonproductive binding to lignin. Biotechnology for biofuels, 6(1), 156. https://doi.org/10.1186/1754-6834-6-156

[66] Wu, W., Li, P., Huang, L., Wei, Y., Li, J., Zhang, L., & Jin, Y. (2023). The role of lignin structure on cellulase adsorption and enzymatic hydrolysis. Biomass, 3(1), 96-107. https://doi.org/10.3390/biomass3010007

[67] Sun, Y., & Cheng, J. (2002). Hydrolysis of lignocellulosic materials for ethanol production: a review. Bioresource technology, 83(1), 1-11. https://doi.org/10.1016/S0960-8524(01)00212-7

[68] Khanam, S., Ray, S. K., Bhuiyan, R. H., Sultana, S., Sharmin, N., & Ehsan, Q. (2025). Advancing nutrient management in agriculture: Rice straw to nitrogen, phosphorus and potassium-containing hydrogel as slow-release fertilizer. Industrial Crops and Products, 224, 120380. https://doi.org/10.1016/j.indcrop.2025.121170

[69] Khanam, S., Yeasmin, F., Mondal, A. K., Naim, M. R., Chowdhury, A., & Ray, S. K. (2025). Redox-driven ultrafast synthesis of lignin-based hydrogel: Optimization, characterization and prospects for slow NPK-fertilizer release under varied environmental conditions. Industrial Crops and Products, 237, 122199. https://doi.org/10.1016/j.indcrop.2025.122199

[70] Khanam, S., Eti, S. A., Bashar, M. S., Sujan, S. A., Sharmin, N., & Ray, S. K. (2025). Dynamic absorption of heavy metal from aqueous solution using lignin-hydrogel and natural filter materials in a packed column system. International Journal of Biological Macromolecules, 302, 140356. https://doi.org/10.1016/j.ijbiomac.2025.140356

Supplementary Files

This is a list of supplementary files associated with this preprint. Click to download.

- SupplimentaryInformation.docx